The natural frequency of oscillation of gas bubbles in tubes

H. N. Oğuz and A. Prosperetti
Department of Mechanical Engineering, The Johns Hopkins University, Baltimore, Maryland 21218

(Received 28 July 1997; accepted for publication 27 February 1998)

A numerical study is presented of the natural frequency of the volume oscillations of gas bubbles in a liquid contained in a finite-length tube, when the bubble is not small with respect to the tube diameter. Tubes rigidly terminated at one end, or open at both ends, are considered. The open ends may be open to the atmosphere or in contact with a large mass of liquid. The numerical results are compared with a simple approximation in which the bubble consists of a cylindrical mass of gas filling up the cross section of the tube. It is found that this approximation is very good except when the bubble radius is much smaller than that of the tube. An alternative approximate solution is developed for this case. The viscous energy dissipation in the tube is also estimated and found generally small compared with the thermal damping of the bubble. This work is motivated by the possibility of using gas bubbles as actuators in fluid-handling microdevices. © *1998 Acoustical Society of America.* [S0001-4966(98)02606-X]

PACS numbers: 43.35.Pt [HEB]

INTRODUCTION

An extensive literature exists on the small-amplitude volume oscillations of gas bubbles in unbounded liquids, near rigid plane boundaries and free surfaces (see, e.g., Strasberg, 1953; Howkins, 1965; Blue, 1966; Plesset and Prosperetti, 1977; Apfel, 1981; Scott, 1981; Prosperetti *et al.*, 1988; Oğuz and Prosperetti, 1990; Prosperetti, 1991). The case of bubbles confined in channels and tubes, however, does not seem to have been considered before except in a brief unpublished report by Devin (1961). Of course, when the radius of the tube is much larger than the bubble—as would be the case, for example, for bubbles entrained in ordinary macroscopic flows—the results for bubbles in unbounded liquids can be used to a good approximation. In the situations of concern here, however, the size of the bubble is not small and the effect of the proximity of the boundary very significant.

The situations considered in this paper are all axisymmetric and are sketched in Fig. 1. The bubble is inside a liquid-filled, finite-length, rigid-walled tube that may be open at both ends [Fig. 1(a), (a′), and (b)], or rigidly terminated at one end and open at the other [Fig. 1(c) and (d)]. The open end(s) of the tube may be in contact with the atmosphere [Fig. 1(b) and (d)], or with a large mass of the same liquid [Fig. 1(a), (a′), and (c)].

Our interest in these problems is motivated by the possibility to use gas bubbles as actuators in the small fluid-handling systems that advances in silicon manufacturing technology are rendering possible (see, e.g., Fujita and Gabriel, 1991; Lin *et al.*, 1991; Gravesen *et al.*, 1993). These include bioassay chips, integrated micro-dosing systems, miniaturized chemical analysis systems, and others. The advantage of bubbles in this setting would be the possibility to power them remotely by ultrasonic beams with no need for direct contact between the actuator and the power supply. A particularly intriguing possibility in this regard may be offered by the ability of ultrasound to propagate through living tissue.

While the scale that we envisage is of the order of one millimeter or less and the flow velocities relatively small, so that viscous effects would not be negligible, it seems natural for a first analysis of this problem to start from a consideration of the inviscid case, treating viscous effects in an approximate way (see Sec. IV). The attending simplification enables us to focus with greater clarity on the inertial aspects of the bubble–fluid interaction, which are one of the dominant aspects of the system. Second, it will be easier to establish a connection with the available results for the unbounded case. Third, one can envisage situations in which viscosity is indeed negligible, such as an oscillation frequency so large that the viscous boundary layer is much thinner than the tube.

Since, in order to maximize the effectiveness of the actuator, it is desirable to operate near resonance conditions, the natural frequency of the bubble is the most significant quantity to be determined. This is the objective of this paper. In the future we shall consider forced oscillations, damping mechanisms, and nonlinear effects.

I. FORMULATION

As shown by Strasberg (1953; see also Oğuz and Prosperetti, 1990), it is possible to obtain a relation for the natural frequency directly by using the analogy with the capacitance problem of electrostatics. To this end we start from the condition expressing the balance of normal forces at the bubble surface:

$$p_i = p_L + \sigma \mathscr{C}. \tag{1}$$

Here, p_i is the pressure in the bubble, assumed spatially uniform, p_L the pressure in the liquid at the bubble surface, σ the surface tension coefficient, and $\mathscr{C}$ the local curvature of the interface. Upon using the (linearized) Bernoulli integral to express p_L in terms of the velocity potential ϕ and the

 0001-4966/98/103(6)/3301/8/$10.00

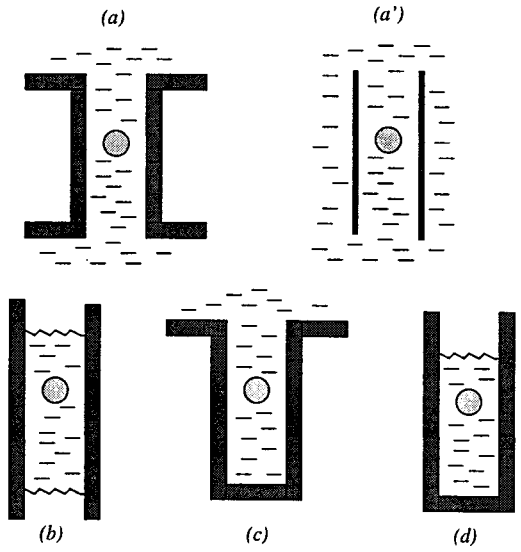

FIG. 1. The various configurations of a bubble in a tube considered in this paper: (a) open tube with infinite thickness immersed in an unbounded liquid; (a) open tube with negligible thickness immersed in an unbounded liquid; (b) partially filled tube with liquid surfaces exposed to the atmosphere; (c) rigidly terminated tube in the bottom of a large container; (d) partially filled tube closed at one end.

static pressure p_∞, the previous relation becomes

$$p_i = -\rho \frac{\partial \phi}{\partial t} + p_\infty + \sigma \mathscr{C}, \tag{2}$$

where ρ is the liquid density. The bubble internal pressure p_i can be assumed to remain spatially uniform at all times. Since p_∞ is a constant, this equation implies then that ϕ will remain essentially uniform over the bubble surface provided it is uniform (e.g., equal to zero) at the initial time, and provided the surface curvature is either uniform or small. The former possibility prevails in the case of small bubbles, which tend to remain spherical, while the latter one is encountered for large bubbles for which the surface tension contribution is negligible. Upon balancing variations in curvature and variations in internal pressure, it is found that the appropriate scale to judge whether a bubble is to be considered ''small'' or ''large'' is of the order of σ/p_∞ which, for the case of water at atmospheric pressure, is a few micrometers.

With the assumption of a uniform internal pressure, averaging Eq. (2) over the bubble surface, we have

$$p_i = -\rho \left\langle \frac{\partial \phi}{\partial t} \right\rangle + p_\infty + \sigma \langle \mathscr{C} \rangle, \tag{3}$$

where $\langle ... \rangle$ denotes the surface average. In the linear approximation, to which we confine ourselves, the surface average of any first-order quantity can consistently be calculated on the unperturbed equilibrium surface, rather than on the moving one. As a consequence, time differentiation and surface averaging commute and therefore, upon differentiating once more with respect to time, we find

$$\rho \frac{d^2}{dt^2} \langle \phi \rangle = -\frac{dp_i}{dt} + \sigma \frac{d}{dt} \langle \mathscr{C} \rangle. \tag{4}$$

For linear oscillations at a single frequency ω, any variable is proportional to any other so that we may write

$$\frac{dp_i}{dt} = \frac{dp_i}{dV} \frac{dV}{dt}, \tag{5}$$

where V is the instantaneous bubble volume and dp_i/dV a possibly complex constant. Furthermore,

$$\frac{dV}{dt} = \int_S \mathbf{u} \cdot \mathbf{n} \, dS \equiv S \left\langle \frac{\partial \phi}{\partial n} \right\rangle, \tag{6}$$

where $\mathbf{n}$ is the outward directed unit normal to the bubble surface S. With the neglect of gravity, the equilibrium configuration of the bubble is necessarily spherical, although the instantaneous shape during volume oscillations is not necessarily so. However, again in the linear approximation, it is easy to show that

$$\frac{d}{dt} \langle \mathscr{C} \rangle = \langle \mathscr{C}_0 \rangle \left\langle \frac{\partial \phi}{\partial n} \right\rangle, \tag{7}$$

where $\langle \mathscr{C}_0 \rangle = 2/a$ is the curvature of a spherical bubble of radius a. Upon substituting these results into Eq. (4), and further writing $i\omega$ for d/dt, we find

$$\omega^2 = -\frac{1}{\rho} \left(S \frac{dp_i}{dV} + \frac{2\sigma}{a^2} \right) \frac{1}{\langle \phi \rangle} \left\langle \frac{\partial \phi}{\partial n} \right\rangle. \tag{8}$$

For a spherical bubble in an infinite liquid $\phi = (a^2/r) \times (da/dt)$ (where r is the distance from the bubble center and da/dt the radial velocity) and this expression reduces to

$$\omega_0^2 = -\frac{1}{a\rho} \left(S \frac{dp_i}{dV} + \frac{2\sigma}{a^2} \right), \tag{9}$$

where ω_0 denotes the bubble angular frequency in this case. Upon taking the ratio with Eq. (8) and introducing the frequencies $f = \omega/2\pi$, $f_0 = \omega_0/2\pi$, we thus have

$$\left(\frac{f}{f_0} \right)^2 = \frac{a}{\langle \phi \rangle} \left\langle \frac{\partial \phi}{\partial n} \right\rangle, \tag{10}$$

which expresses in a compact form the change in the natural frequency of the bubble due to the presence of boundaries. The validity of this result presupposes of course that dp_i/dV in Eq. (8) has the same value as for a bubble in an infinite fluid. This assumption may be justified as follows. The rate of change of the internal pressure with volume is determined essentially by the thermal processes in the bubble. It is well known that, to an excellent approximation, these can be evaluated assuming the bubble surface temperature to remain undisturbed (see, e.g., Kamath *et al.*, 1993), which effectively decouples the thermal problem from the environment surrounding the bubble.

If the length of the tube were infinite, volume changes of the bubble would only be possible in a compressible fluid. However, if the length of the tube is much smaller than the wavelength of sound in the liquid, we may use the incompressible approximation so that the velocity potential satisfies Laplace's equation $\nabla^2 \phi = 0$. For simplicity we only consider axisymmetric situations. The boundary condition on the surrounding solid boundaries is of course $\mathbf{n} \cdot \nabla \phi = 0$. If the liquid mass in the tube is bounded by a free surface in con-

tact with the atmosphere, as in Fig. 1(b) and (d), $\phi=0$ is the appropriate boundary condition there. Furthermore, unless the bubble is very close to this surface, there will be little error in assuming it to be plane. If, on the other hand, the tube is part of an extended (infinite) mass of liquid, as in Fig. 1(a), (a′), and (c), ϕ is required to vanish at infinity.

As noted before, provided the bubble is either relatively small or relatively large, one may assume that ϕ remains uniform over the bubble surface. Since the problem for ϕ is linear and, aside from the boundary condition on the bubble surface, it is homogeneous, it follows that $\langle \partial\phi/\partial n \rangle$ will also be proportional to the average value of ϕ evaluated on the bubble surface. It is therefore sufficient to calculate the surface averages appearing in Eq. (10) by solving Laplace's equation subject to the boundary condition $\phi=1$ on the undisturbed spherical bubble.

The solution of the potential problem formulated before can readily be obtained by using the boundary integral method (see, e.g., Pozrikidis, 1992). Our version of this method is already well documented in the literature, to which the reader is referred (see, e.g., Oğuz and Prosperetti, 1990).

The derivation of the numerical results shown below, the accuracy of which was verified by the standard convergence and grid-independence tests, did not require a very high degree of discretization. The line representing the bubble surface in the meridian plane was approximated by cubic splines with 10 nodal points. Up to 70 points were used on the tube's wall, depending on its length. In situations where the solid boundary extends to infinity [Fig. 1(a) and (c)], the integration over its surface must be stopped at some large distance from the axis of symmetry. Ten tube radii proved sufficient for convergence.

II. APPROXIMATIONS

The numerical calculation of the natural frequency according to the method described before is a matter of some complexity and it is useful therefore to obtain approximate expressions. We consider separately the case of large and small bubbles.

A. Large bubbles

When the radius a of the bubble is not small compared with the radius R of the tube, an obvious approximation to the situation envisaged here is that of a one-dimensional ''slice'' of gas filling the entire cross section of the tube and with a thickness h adjusted to give the same volume as the real bubble:

$$Ah=\tfrac{4}{3}\pi a^3, \tag{11}$$

where A is the tube's cross sectional area. Since the considerations that follow are applicable to tubes of general cross section, we do not specialize the formulae to circular tubes in this subsection.

Let the bubble center be at a distance L_1 from one end of the tube and $L_2=L-L_1$ from the other. For greater accuracy, these geometrical parameters can be adjusted to reflect more closely the physical situation. In the first place, in order to preserve the total volume, an amount

$$l=\frac{1}{2}\,h=\frac{2}{3}\,\pi\,\frac{a^3}{A} \tag{12}$$

must be subtracted from both L_1 and L_2. If the tube's ends are in contact with the atmosphere [Fig. 1(b) and (d)], this is the only adjustment to the lengths of the liquid columns. If an end is immersed in an unbounded liquid [Fig. 1(a), (a′), and (c)], however, there is an added mass effect that can be accounted for by augmenting the geometrical length by an amount ΔL. For the situation of Fig. 1(a) one can simply estimate this end correction by noting that, from the point of view of the fluid outside the tube, the effect of the liquid entering and exiting the tube opening is similar to the pulsations of a ''half-bubble'' with diameter equal to the hydraulic diameter D_h of the tube. (The hydraulic diameter is four times the ratio of the cross-sectional area A to the perimeter P of the tube.) Since such a bubble in an unbounded liquid would have an added, or virtual, mass $4\pi(D_h/2)^3\rho$, the added mass for the half-bubble is $2\pi(D_h/2)^3\rho$, which can be accounted for by extending the tube by an amount ΔL chosen so that $A\Delta L$ contains an equal mass of liquid. The result is

$$\Delta L=16\pi\,\frac{A^2}{P^3}, \tag{13}$$

and equals $2R$ for a circular tube. This result can also be derived in an alternative, more rigorous way (Oğuz and Zeng, 1995, 1997). The same procedure applied to the thin-walled tube of Fig. 1(a′) is inaccurate, however, as shown by Levine and Schwinger (1948). In this case, for a circular tube, one finds $\Delta L\simeq 1.22R$.

On the basis of these arguments we define equivalent lengths of the liquid columns on the two sides of the bubble by

$$L_i^e=L_i-l+\Delta L, \quad i=1,2. \tag{14}$$

If the system is regarded as an oscillator, its equivalent mass is [see Eq. (33) in Sec. IV]:

$$M_{\rm eq}=\rho A\left(\frac{1}{L_1^e}+\frac{1}{L_2^e}\right)^{-1}, \tag{15}$$

while the ''spring constant'' is

$$K=-A^2\,\frac{dp_i}{dV}. \tag{16}$$

The natural frequency of the system is therefore

$$\omega_a^2=\frac{K}{M_{\rm eq}}=-\left(\frac{1}{L_1^e}+\frac{1}{L_2^e}\right)\frac{A}{\rho}\,\frac{dp_i}{dV}. \tag{17}$$

With $f_a=\omega_a/2\pi$, upon taking the ratio of this expression to the natural frequency of a bubble of equal radius in an unbounded liquid (neglecting surface tension effects), we find

$$\left(\frac{f_a}{f_0}\right)^2=\frac{A}{4\pi a}\left(\frac{1}{L_1^e}+\frac{1}{L_2^e}\right). \tag{18}$$

If one of the ends is rigidly terminated, we assume that the liquid on that side does not partake of the motion in this one-dimensional approximation. This limit is contained in

the previous formulae by taking the corresponding effective length to be infinite. It will be seen in the next section that this is a good approximation.

B. Small bubbles

The model just described is evidently a poor approximation when the bubble is small compared with the tube radius. We now turn to this case considering explicitly a tube open at the two ends. The adjustment (14) to the length of the liquid columns permits one to adapt the results to the other cases depicted in Fig. 1.

It is particularly convenient to use the following special representation of the velocity potential:

$$\phi=\sum_{n=0}^{\infty} A_n \frac{a^{n+1}}{\rho^{n+1}} P_n(\cos\,\theta)+\sum_{n=1}^{\infty} B_n I_0\left(\frac{n\pi r}{L}\right)\sin\frac{n\pi z}{L} + C_0\frac{z}{L}+D_0\frac{L-z}{L}+\sum_{n=1}^{\infty}\left[C_n\frac{\sinh\,\alpha_n(z/R)}{\sinh\,\alpha_n(L/R)} + D_n\frac{\sinh\,\alpha_n(L-z)/R}{\sinh\,\alpha_n(L/R)}\right]J_0\left(\alpha_n\frac{r}{R}\right). \tag{19}$$

Here the P_n's are Legendre polynomials, and ρ and θ are polar coordinates centered at the bubble center; r and z are cylindrical coordinates with the two free surfaces of the liquid at $z=0$ and $z=L$. The modified and ordinary Bessel functions of order 0 are denoted by I_0 and J_0, the α_n's are the zeros of J_1, and the coefficients A_n, B_n, C_n, D_n are to be determined from the boundary conditions. This particular form for ϕ is constructed in such a way that the first summation describes the flow near the bubble, the second one in the tube away from the bubble, the next two terms the bulk translation of the liquid away from the bubble, and the last summation the end effects. The proof that Eq. (19) gives an accurate representation of the potential follows from the fact that, as will be seen shortly, all the coefficients are uniquely determined and all the boundary conditions are satisfied.

On the tube wall the velocity must vanish, which requires

$$\frac{\partial}{\partial r}\sum_{n=0}^{\infty} A_n\frac{a^{n+1}}{\rho^{n+1}}P_n(\cos\,\theta) + \sum_{n=1}^{\infty} B_n\frac{n\pi}{L}I_1\left(\frac{n\pi R}{L}\right)\sin\frac{n\pi z}{L}=0. \tag{20}$$

At the lower and upper free surfaces of the tube, $z=0$ and $z=L$, the condition of vanishing pressure perturbation simply requires $\phi=0$, i.e.,

$$\sum_{n=0}^{\infty} A_n\frac{a^{n+1}}{\rho^{n+1}}P_n(\cos\,\theta)+\sum_{n=1}^{\infty} D_n J_0\left(\alpha_n\frac{r}{R}\right)+D_0=0, \tag{21}$$

$$\sum_{n=0}^{\infty} A_n\frac{a^{n+1}}{\rho^{n+1}}P_n(\cos\,\theta)\sum_{n=1}^{\infty} C_n J_0\left(\alpha_n\frac{r}{R}\right)+C_0=0. \tag{22}$$

A consideration of these boundary conditions furnishes a rationale for the representation (19) of the potential. Indeed, from these three homogeneous boundary conditions one can conceptually think of expressing B_n, C_n, and D_n in terms of the A_n, which are in turn determined by the pressure condition on the bubble surface.

If the bubble radius is small, the magnitude of the higher-order terms of the Legendre polynomial expansion is rapidly decreasing and therefore we truncate this infinite sum to just the first term which, in the cylindrical coordinate system used to express the other terms, is

$$A_0\frac{a}{\rho}P_0=A_0\frac{a}{[r^2+(z-d)^2]^{1/2}}, \tag{23}$$

where d is the position of the bubble center. Using well-known orthogonality properties we then have from Eqs. (20) to (22):

$$\frac{B_n}{A_0}=\frac{2}{n\pi}\frac{1}{I_1(n\pi R/L)}\int_0^L\frac{R}{[R^2+(z-d)^2]^{3/2}}\sin\left(\frac{n\pi z}{L}\right)dz, \tag{24}$$

$$\frac{D_0}{A_0}=-\frac{2}{R^2}\int_0^R\frac{r}{\sqrt{r^2+d^2}}\,dr, \tag{25}$$

$$\frac{D_n}{A_0}=-\frac{2}{R^2J_0^2(\alpha_n)}\int_0^R\frac{r}{\sqrt{r^2+d^2}}J_0\left(\alpha_n\frac{r}{R}\right)dr, \tag{26}$$

$$\frac{C_0}{A_0}=-\frac{2}{R^2}\int_0^R\frac{r}{\sqrt{r^2+(L-d)^2}}\,dr, \tag{27}$$

$$\frac{C_n}{A_0}=-\frac{2}{R^2J_0^2(\alpha_n)}\int_0^R\frac{r}{\sqrt{r^2+(L-d)^2}}J_0\left(\alpha_n\frac{r}{R}\right)dr. \tag{28}$$

In principle, A_0 should now be determined by imposing a condition on $\langle\phi\rangle$ at the bubble surface. As is evident from the previous relations, however, all the coefficients are proportional to A_0 and it will be recalled from Eq. (10) that we are only interested in the ratio $(1/\langle\phi\rangle)\langle\partial\phi/\partial n\rangle$ that is obviously independent of A_0. It is therefore unnecessary to impose the last boundary condition explicitly and A_0 can simply be taken as 1.

Of course, it is not necessary to truncate the spherical harmonic expansion in Eq. (19) at the first term. In principle, one can retain any number of terms in the sums. Upon taking scalar products, one is then reduced to a linear system for the coefficients. As discussed in the next section, we have found that the truncation used here is sufficient for the present purposes of approximation. Solution (19), however, is in principle exact and represents a valid alternative to the boundary integral calculation, at least for situations of the type shown in Fig. 1(b) and (d). It is interesting to note that this procedure can be extended to deal with bubbles off-axis, and tubes of noncircular cross section, more simply than the boundary integral method.

Devin (1961) calculated the natural frequency for the situation of Fig. 1(a′) in terms of the potential and kinetic energies of the system. The former is simply expressed in terms of the relation between the pressure and volume of the bubble, which he assumed to be adiabatic. To estimate the kinetic energy, he used the solution for a point source in an

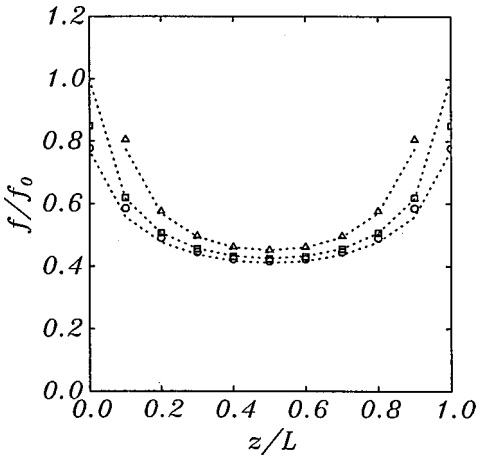

FIG. 2. The natural frequency of a bubble of radius a in a tube of radius R and length L as a function of the axial distance of the bubble center from the tube bottom for $L/R=10$, $a/R=0.5$. The dotted lines show the result given by the approximate formula (18) and the symbols show the boundary integral results; ○ case of Fig. 1(a); □ case of Fig. 1(a′); △ case of Fig. 1(b).

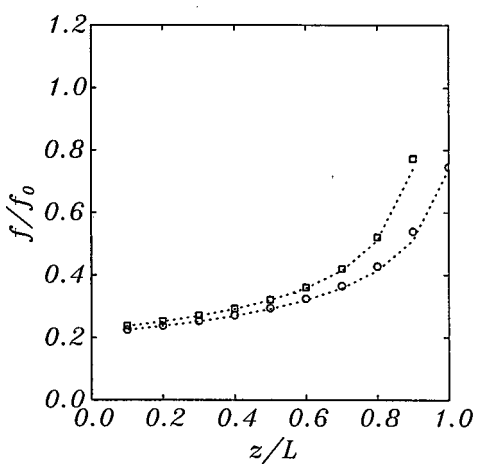

FIG. 3. The natural frequency of a bubble of radius a in a tube of radius R and length L as a function of the axial distance of the bubble center from the tube bottom for $L/R=10$, $a/R=0.5$. The dotted lines show the result given by the approximate formula (18) and the symbols show the boundary integral results; ○ case of Fig. 1(c); □ case of Fig. 1(d).

infinite tube up to a distance of 1.108 R from the bubble center (at which point the potential along the axis vanishes) combined with that of solid-body motion of the liquid in the remainder of the tube. His argument for chosing the particular value 1.108 is that, in this way, ''the decrease in the tube potential from the surface of the bubble... is exactly equal to the decrease in the free field potential from the surface of an identical bubble to a point at infinity.'' His final result is

$$\left(\frac{f_D}{f_0}\right)^2=\left[1+\frac{2a}{R}\left(\frac{\frac{1}{2}L+\Delta L}{R}-1.108\right)\right]^{-1}. \tag{29}$$

Here the bubble is assumed to be located at the midpoint of the tube and $\Delta L\simeq 1.22R$. It is evident from the manner of its derivation that the result is only applicable provided the bubble radius is much smaller than that of the tube, and that the term in brackets is greater than 1.

III. RESULTS

Any one of the situations shown in Fig. 1 is characterized by four dimensional lengths: the bubble radius a, the tube radius R, the tube length L, and the distance of the bubble center from the lower end of the tube (as sketched in Fig. 1), z. [In the case of Fig. 1(a′), the tube thickness would also appear, but we take it as negligibly small in the following.] One can thus form three dimensionless ratios that fully characterize each case. The presentation of a sufficient number of results to cover the entire parameter space is impractical. Thus we limit ourselves to a few examples which also serve to illustrate the excellent performance of the approximations described in the previous section. It may be noted that, by symmetry, a bubble placed at the tube's midpoint in the situations of Fig. 1(a) and (b) is equivalent to a ''half-bubble'' resting on the rigid bottom of Fig. 1(c) and (d) for a tube of half the length.

Figures 2 to 5 show a few representative results. In all these figures the open symbols are the (numerically) exact results obtained with the boundary integral method, the dotted lines are the large-bubble approximation of Sec. II A, and the solid lines the small-bubble approximations of Sec. II B.

Figures 2 and 3 give the ratio f/f_0 as a function of the position of the bubble center along the tube for the five situations depicted in Fig. 1. Here the tube's radius is twice that of the bubble. Figures 4 and 5 are graphs of f/f_0 as a function of a/R for $L/R=10$, again for four of the situations of Fig. 1. Here the bubble center is at the midpoint of the tube axis. The small-bubble approximation of Sec. II B (solid lines) has been evaluated retaining only B_1, C_0, C_1, D_0, and D_1.

The first obvious feature shown by these figures is that the effect of the tube can be large. For example, from Fig. 3, we see that a bubble in a tube closed at one end [Fig. 1(c) and (d)] has a 50% reduction in the natural frequency when the tube radius is twice the bubble radius and the depth of

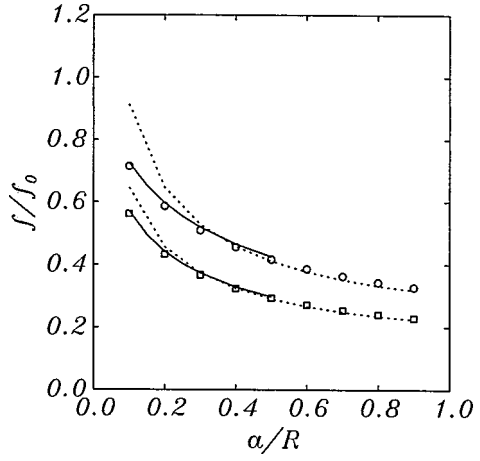

FIG. 4. The natural frequency of a bubble centered at the midpoint of the axis of a tube of radius R and length L as a function of the normalized bubble radius a/R for $L/R=10$. The dotted lines show the result given by the approximate formula (18), the solid lines those given by the small-bubble approximation, and the symbols show the boundary integral results; ○ case of Fig. 1(a); □ case of Fig. 1(c).

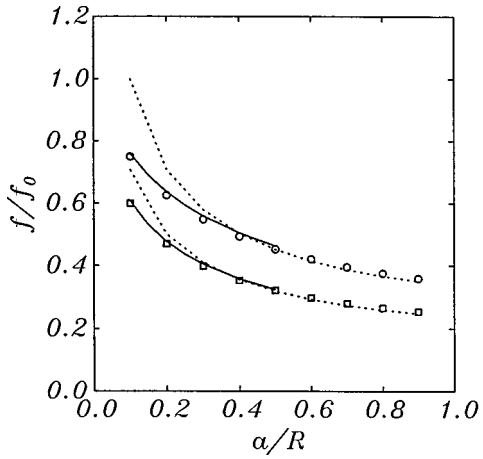

FIG. 5. The natural frequency of a bubble centered at the midpoint of the axis of a tube of radius R and length L as a function of the normalized bubble radius a/R for $L/R=10$. The dotted lines show the result given by the approximate formula (18), the solid lines those given by the small-bubble approximation, and the symbols show the boundary integral results; ○ case of Fig. 1(b); □ case of Fig. 1(d).

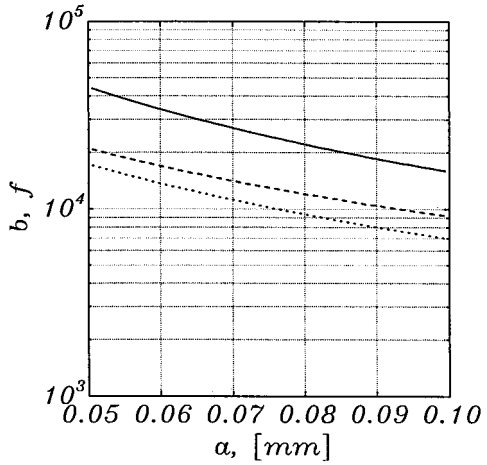

FIG. 7. Natural frequency f in Hz (solid line) and total damping parameter b in s^{-1} [Eq. (40), dashed line] as a function of bubble radius in a tube of radius 0.1 mm and length 1 mm for an air bubble in water. The bubble is positioned at the bottom of the tube. The dotted line is the thermal contribution to the damping. This figure refers to case (d) of Fig. 1 but, with the adjustment to the tube length described in Sec. II A, the results can be adapted to the case of Fig. 1(c) as well.

submergence below the tube mouth is of the order of twice the tube radius.

Another obvious remark suggested by the numerical results is the surprising degree to which the approximations of the previous section are able to reproduce the exact results. In particular, the adjustments to the liquid column length described in Sec. II A are seen to work very well. The large-bubble approximation breaks down around $a/R\simeq 0.2$, while the small bubble model works relatively well at least up to $a/R\simeq 0.5$. It is therefore found that there is a domain in which both approximations are reasonably accurate.

We have examined the effect of retaining more terms in the summations of representation (19) of the velocity potential. The effect of adding two terms to each of the sums is small, and any more terms give differences that are indistinguishable in a graph such as those of Figs. 4 to 7.

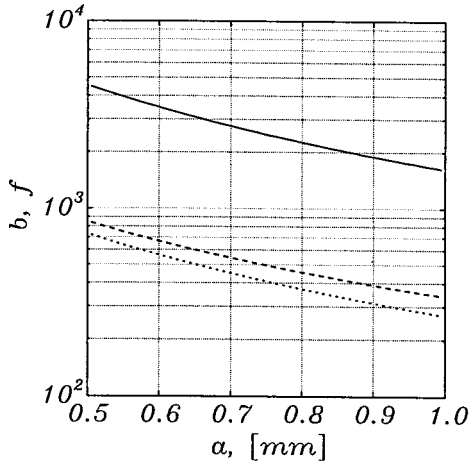

FIG. 6. Natural frequency f in Hz (solid line) and total damping parameter b in s^{-1} [Eq. (40), dashed line] as a function of bubble radius in a tube of radius 1 mm and length 10 mm for an air bubble in water. The bubble is positioned at the bottom of the tube. The dotted line is the thermal contribution to the damping. This figure refers to case (d) of Fig. 1 but, with the adjustment to the tube length described in Sec. II A, the results can be adapted to the case of Fig. 1(c) as well.

In addition to the theoretical development leading to Eq. (29) quoted before, Devin's report contains a few data taken in an experimental setup similar to that of our Fig. 1(a′). The bubbles were generated by a needle placed at the midpoint of the axis of vertical brass cylinders with a diameter of 30 mm, a wall thickness of 3.2 mm, and a length of 120 or 240 mm. In order to investigate the effect of static pressure, two depths of submergence of the tube below the surface of a large water tank were used, 5 and 15 ft. A hydrophone placed at a distance of 0.1 m recorded the sound emitted by the bubbles pinching off the needle and a few graphs of the acoustic power spectral density are shown in the report. By digitizing these figures, we have read off the position of the maximum of these spectra which, in view of the small damping, give a good estimate of the natural frequency. Values of the bubble radius are not given but, in his graphs, Devin shows the natural frequency of the bubble generated by the same method in an unbounded liquid from which the radius can be deduced according to the results of Prosperetti (1991). Table I shows all of Devin's data together with the result given by the first four terms of the series solution of Sec. II B and two estimates obtained from Devin's report. The first one is found from his approximate formula (29), while the second one is the theoretical value read from his graph. These two numbers should agree but, for the first case, we find a 2% discrepancy the origin of which is not clear. This data point also exhibits a greater difference with the theory, about 5%. For the second and third data points agreement with theory is within about 3% and 1%, respectively, and seems to be slightly better for the present theory than for Devin's although, on the basis of the information provided, it is not possible to estimate accurately the error in his data.

TABLE I. Comparison between Devin's data, the present series solution of Sec. II B, and Devin's theory. The tube was brass with a radius of 15 mm.

a (mm)	L (cm)	Exp.	Present theory	Devin, Eq. (29)	Devin, graph
1.51	24	0.67	0.636	0.638	0.653
1.52	12	0.74	0.762	0.777	0.779
1.50	12	0.76	0.764	0.780	0.777

IV. DAMPING RATE

In reality, the oscillations executed by the bubbles shown in Fig. 1 are, of course, damped. In the previous developments we have disregarded dissipative effects which, as is well known, affect the natural frequency only to second order. The decay rate is however a first-order effect, that we now consider.

A bubble oscillating in an unbounded liquid loses energy by thermal conduction across the gas–liquid interface, acoustic radiation, and the action of viscous stresses at the interface. In water, acoustic losses only dominate for bubble radii larger than several millimeters, while viscous losses are significant only for bubbles smaller than about 10 μm. The dominant energy loss for intermediate values of the radius is of thermal origin, and this can be assumed to happen also in the cases of Fig. 1. Indeed, in the underlying process, the significant aspects are the gas volume expansion and contraction and the fact that the bubble surface remains essentially at the undisturbed liquid temperature during the oscillations due to the large thermal capacity of the liquid. Both circumstances occur also in the situations of present concern, as already noted in connection with Eq. (10). In the case of a bubble in a tube, however, a new energy loss mechanism is present, namely viscous dissipation due to liquid flow along the surface of the tube surrounding the bubble. An estimate of the rate of damping due to this effect can be found on the basis of the simple one-dimensional model of Sec. II A as follows.

Consider the bubble as occupying a ''slice'' of the tube extending between $z_1(t)$ and $z_2(t)$. If m_1 and m_2 are the (effective) masses of the two liquid columns, and β_1, β_2 the damping rates due to viscous dissipation, the equations of motion of the two interfaces are

$$m_1\ddot{z}_1+2\beta_1\dot{z}_1+K(z_1-z_2)=0, \tag{30}$$

$$m_2\ddot{z}_2+2\beta_2\dot{z}_2-K(z_1-z_2)=0, \tag{31}$$

with the ''spring constant'' K given by Eq. (16). The equation for the (complex) frequencies of oscillation Ω of this system is readily written down and is

$$\begin{vmatrix} m_1\Omega^2-K-2i\beta_1\Omega & K \\ K & m_2\Omega^2-K-2i\beta_2\Omega \end{vmatrix}=0. \tag{32}$$

Upon setting $\Omega=\omega+ib_t$, up to terms of the first order in β_i, one readily finds

$$\omega^2=K\left(\frac{1}{m_1}+\frac{1}{m_2}\right), \tag{33}$$

which is the same as Eq. (17), and

$$b_t=\frac{1}{m_1+m_2}\left(\beta_1\frac{m_2}{m_1}+\beta_2\frac{m_1}{m_2}\right). \tag{34}$$

In the spirit of Sec. II A, the masses appearing here are given by $m_j=\rho L_j^e A$, $j=1,2$.

To estimate the damping parameters β_i we proceed approximately as follows (disregarding the index i for the moment). The energy dissipated during one cycle by each oscillator is

$$\mathscr{E}_d=2\beta\int_0^{2\pi/\omega}\dot{z}^2\,dt, \tag{35}$$

which furnishes an estimate of β if the other two quantities can be evaluated. Since, to leading order, z oscillates sinusoidally with a frequency ω and velocity amplitude V, the integral has the value $(\pi/\omega)V^2$. The energy loss can be estimated by integrating the dissipation function over the volume occupied by the fluid. With the approximation of periodic, parallel flow, we have

$$\mathscr{E}_d=\mu L\int_0^{2\pi/\omega}dt\int_A dA\left(\frac{\partial u}{\partial r}\right)^2, \tag{36}$$

where μ is the liquid viscosity, the integral is over the cross section of the tube, and u is the axial velocity. Since, in fully developed parallel flow, the problem for u is linear, we have $u\propto V$ and therefore

$$\beta=\frac{\omega}{2\pi}\,\mu L\int_0^{2\pi/\omega}dt\int_A dA\left[\frac{\partial}{\partial r}\left(\frac{u}{V}\right)\right]^2. \tag{37}$$

The velocity field required here is readily calculated from the Navier–Stokes equations (see, e.g., Leal, 1992), but the answer is in terms of Bessel functions with complex argument and it does not appear possible to obtain closed-form expressions for this integral at arbitrary frequency. Approximations for $\sqrt{\mu/\omega\rho}\gg R$ and $\sqrt{\mu/\omega\rho}\ll R$ are, however, readily found. In the first case we have

$$\beta=4m\,\frac{\mu}{\rho R^2}, \tag{38}$$

which can also be obtained from the Poiseuille flow solution, while, in the latter one,

$$\beta=m\sqrt{\frac{\mu\omega}{2\rho R^2}} \tag{39}$$

which, in the spirit of a boundary layer approximation, can also be obtained from the known form of the velocity field over an infinite oscillating flat plate. This latter result is therefore valid for tubes of arbitrary cross section.

The preceding arguments provide an approximation to the viscous damping in the tube b_t. As already mentioned, the gas–liquid heat exchange gives rise to another dissipation mechanism. If the corresponding damping rate is much less than ω, the two damping mechanisms are additive and the total damping of the oscillations is therefore

$$b = b_t + b_b, \tag{40}$$

where b_b is the bubble damping constant that has been exhaustively studied in the literature (see, e.g., Prosperetti *et al.*, 1988; Prosperetti, 1991).

To illustrate the magnitude of the effect, we consider two particular cases in Figs. 6 and 7. These figures refer to the situation of Fig. 1(d) for an air bubble in water at 1 atm but, with the adjustment to the tube length described in Sec. II A, the results are also representative of case 1(c). In Fig. 6 the tube has a length of 10 mm and a radius of 1 mm, while in Fig. 7 the corresponding values are 1 and 0.1 mm, respectively. The bubble is positioned at the bottom of the tube (in the sense of the approximate conceptual model of Sec. II A; strictly speaking, therefore, the radius shown is an equivalent spherical radius). The horizontal axis shows the bubble radius, the solid line the natural frequency, the dotted line the thermal damping, and the dashed line the total damping. The viscous contribution is just the difference between the two lines, and is therefore seen to be small in both cases. Just as in the case of a bubble in an unbounded fluid, we thus see that thermal damping is the dominant mechanism of energy dissipation.

ACKNOWLEDGMENTS

The authors are grateful to Dr. Murray Strasberg for calling their attention to Devin's work on this problem. Thanks are also due to X. M. Chen for her help with the calculations of Sec. IV. This study has been supported by the Air Force Office of Scientific Research under Grant No. F49620-96-1-0386.

Apfel, R. E. (**1981**). *Acoustic Cavitation,* in *Methods of Experimental Physics—Vol. 19 Ultrasonics*, edited by P. D. Edmonds (Academic, New York), pp. 355–411.

Blue, J. E. (**1966**). ''Resonance of a bubble on an infinite rigid boundary,'' J. Acoust. Soc. Am. **41**, 369–372.

Devin, C. (**1961**). ''Resonant frequencies of pulsating air bubbles generated in short, open-ended pipes,'' Technical Report 1522, David Taylor Model Basin, Hydromechanics Laboratory.

Fujita, H., and Gabriel, K. J. (**1991**). ''New opportunities for micro actuators,'' in *Transducers '91* (IEEE, New York), pp. 14–20.

Gravesen, P., Branebjerg, J., and Jensen, O. S. (**1993**). ''Microfluidics—A review,'' J. Micromech. Microeng. **3**, 168–182.

Howkins, S. D. (**1965**). ''Measurements of the resonant frequency of a bubble near a rigid boundary,'' J. Acoust. Soc. Am. **37**, 504–508.

Kamath, V., Prosperetti, A., and Egolfopoulos, F. (**1993**). ''A theoretical study of sonoluminescence,'' J. Acoust. Soc. Am. **93**, 248–260.

Lin, L., Pisano, A. P., and Lee, A. P. (**1991**). ''Microbubble powered actuator,'' in *Transducers '91* (IEEE, New York), pp. 1041–1044.

Leal, L. Gary (**1992**). *Laminar Flow and Convective Transport Processes, Scaling Principles and Asymptotic Analysis* (Butterworth-Heinemann, Boston).

Levine, H., and Schwinger, J. (**1948**). ''On the radiation of sound from an unflanged circular pipe,'' Phys. Rev. **73**, 383–405.

Oğuz, H. N., and Zeng, J. (**1995**). ''Boundary integral simulations of bubble growth and detachment in a tube,'' in *Boundary Elements XVII* (Computational Mechanics Publications, Madison, WI), pp. 645–652.

Oğuz, H. N., and Zeng, J. (**1997**). ''Axisymmetric and three-dimensional boundary integral simulations of bubble growth from an underwater orifice,'' Engineering Analysis with Boundary Elements **19**, 313–330.

Oğuz, H. N., and Prosperetti, A. (**1990**). ''Bubble entrainment by the impact of drops on liquid surfaces,'' J. Fluid Mech. **219**, 143–179.

Plesset, M. S., and Prosperetti, A. (**1977**). ''Bubble dynamics and cavitation,'' Annu. Rev. Fluid Mech. **9**, 145–185.

Pozrikidis, C. (**1992**). *Boundary Integral and Singularity Methods for Linearized Viscous Flow* (Cambridge U.P., Cambridge).

Prosperetti, A., Crum, L. A., and Commander, K. W. (**1988**). ''Nonlinear bubble dynamics,'' J. Acoust. Soc. Am. **83**, 502–514.

Prosperetti, A. (**1991**). ''The thermal behaviour of oscillating gas bubbles,'' J. Fluid Mech. **222**, 587–616.

Scott, J. F. (**1981**). ''Singular perturbation theory applied to the collective oscillation of gas bubbles in a liquid,'' J. Fluid Mech. **113**, 487–511.

Strasberg, M. (**1953**). ''The pulsation frequency of nonspherical gas bubbles in liquids,'' J. Acoust. Soc. Am. **25**, 536–537.